Tribology International 163 (2021) 107189

Contents lists available at ScienceDirect

Tribology International

journal homepage: www.elsevier.com/locate/triboint

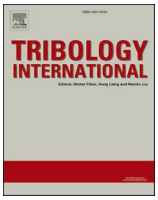

Double hybrid lubricant additives consisting of a phosphonium ionic liquid and graphene nanoplatelets/hexagonal boron nitride nanoparticles

Khodor I. Nasser, José M. Liñeira del Río, Fátima Mariño, Enriqueta R. López, Josefa Fernández *

Laboratorio de Propiedades Termofísicas y Tribológicas, Grupo Nafomat, Departamento de Física Aplicada, Facultad de Física, Universidade de Santiago de Compostela, 15782 Santiago de Compostela, Spain

ARTICLE INFO

Keywords:
Lubricant additive
Nanomaterials
Ionic liquids
Hybrid additives

ABSTRACT

Tribological performance of polyalphaolefin 32, PAO, is investigated by adding two nanomaterials (graphene nanoplatelets, GnP, and hexagonal boron nitride nanoparticles, h-BN) and an ionic liquid ([$P_{6,6,6,14}$][DEHP], IL1, [$P_{2,4,4,4}$][DEP], IL2, or [$P_{6,6,6,14}$][$(iC8)_2PO_2$], IL3). Designed double hybrid nanodispersions are PAO/1 wt% ILX/0.05 wt% GnP/0.1 wt% h-BN (X = 1, 2 or 3). The best anti-friction behavior corresponds to PAO/IL3/GnP/h-BN (40% reduction compared to that achieved with PAO). Anti-wear behavior is similar for the three double hybrid nanodispersions. Roughness of the worn surface tested with PAO is higher than that obtained for each of the nanodispersions. Tribo-film formation and repair effect on worn surfaces due to ILs and nanoparticles are revealed. Some positive synergies were found between each IL and GnP/h-BN as hybrid PAO additives.

1. Introduction

Reducing friction and wear is a global challenge, as both occur in an ever-increasing variety of material applications, from simple devices to industrial machinery components. Total world energy consumption coming from tribological contacts is around 23% [1]. Diminishing friction and wear is an important task not only to save energy, but also to extend the life of mechanical apparatus and reduce emissions [2–4].

Lubrication is one of the best useful ways to manage friction and wear, which is meaningful for energy saving, air pollution control and environmental protection [1–3]. For this reason, extensive research should be ongoing to develop high-performance lubricants. Nowadays, in boundary lubrication regime, controlled addition of nanoparticles (NPs) can tune the lubrication performance of oil-based lubricants, because NPs might enter the tribological contact area enhancing the tribo-film performance [5–8]. Their nanometric size allows them to fill friction interfaces and act as friction modifiers as well as extreme pressure and anti-wear additives [6]. Several mechanisms are proposed as causes of friction and wear reductions due to NPs: mending effect, ball bearing effect, rolling effect or protective tribo-film effect [9–11]. Soft metallic NPs can produce a protective film, thus reducing friction and wear [5,12,13]. Tribo-films allow a smooth operation of mechanical devices with less friction preventing scuffing. On the other hand, two sliding surfaces can be separated by hard NPs, increasing their load-bearing capacity. In addition, the anti-wear effect can also be achieved due to mending effect on the worn surfaces due to nanoparticles, which fill surface grooves and/or adhere to the worn surface [14]. In this last mechanism, also known as surface repairing effect, NPs can repair the surface defects induced by friction, leading to both a reduction in the roughness of rubbing surfaces and the improvement of tribological properties [15].

Another important method to improve the lubrication performance of lubricant oils is the use of ionic liquids (ILs) as additives, which have extremely desirable attributes when used in the formulation of advanced lubricants [16,17]. In the early days, ILs were used as neat lubricants demonstrating very good tribological performance for many different chemical structures [16,18]. Because of their intrinsic polarity, ILs are firmly adsorbed on the metallic surfaces leading to strong tribo-films. Generally, the tribo-film on the contact surfaces is due to the selective adsorption of the IL anion/cation pair onto the metallic contact pair, providing reductions in friction and wear [19]. This tribo-film also provides enhanced resistance to scuffing for longer time under poor lubrication conditions. Nonetheless, the use of ILs as neat lubricants is limited to critical applications due to their high price compared to traditional base oils. For this reason and because small amounts of ILs (1–5 wt%) can significantly improve the tribological performance of the

* Corresponding author.
E-mail address: josefa.fernandez@usc.es (J. Fernández).

https://doi.org/10.1016/j.triboint.2021.107189
Received 27 May 2021; Received in revised form 2 July 2021; Accepted 12 July 2021
Available online 14 July 2021

base oil, ILs are used as lubricating additives [14,20–22].

Therefore, ILs and nanoparticles play an important role in improving the performance of the lubrication oils, whether they are used separately as individual additives or in formulating hybrid combinations [23–26]. Thus, the addition of both NPs and ILs to base oils can significantly improve the tribological properties compared to traditional lubricants, increasing their anti-friction and anti-wear performance [25,27–30]. These combinations allow increasing the stability of nanomaterials as additives in oils and particularly for traditional lubricants in which these additives cannot be easily dispersed [27]. This hybrid addition can lead to a better tribological behavior of the lubricant due to the synergistic lubrication effect, the mechanisms of which are not well-known [31]. On the other hand, the combination of different types of nanomaterials as additives recently opened new opportunities for the development of lubricants with excellent tribological performances due to the positive synergies among two or more components [5,32–35].

Combining the positive synergistic effect that two different nano-additives can display, with the good tribological behavior of ILs as additives, the idea of IL/NP1/NP2 hybrid additives arose. Thus, IL/NP1/NP2 additives could be considered a great enhancer of the tribological properties of lubricants, but, up to our knowledge, no studies have been carried out on this matter. This research proposes to merge the capabilities of the IL/NP and NP1/NP2 combinations that is, the double hybrid combination IL/NP1/NP2, as anti-friction and anti-wear enhancers. With this aim, in this work two different nanomaterials, hexagonal boron nitride nanoparticles (h-BN) and graphene nanoplatelets (GnP), combined with three phosphonium ILs, $[P_{6,6,6,14}][DEHP]$ (IL1), $[P_{2,4,4,4}][DEP]$ (IL2) or $[P_{6,6,6,14}][(iC8)_2PO_2]$ (IL3), are studied as double hybrid additives of polyalphaolefin 32 (PAO). This polyalphaolefin has been chosen because it is one of the most widely used lubricant bases in current oil formulations of wind turbine gearboxes [36,37]. Taking into account that the highest source of energy loss in the gearboxes comes from friction between meshing teeth [36], the use of high performance gearbox oils seems to be a very simple way to reduce power losses [37]. PAOs, saturated hydrocarbons classified by the American Petroleum Institute as group IV base oils [38] and named for their kinematic viscosity at 373.15 K, are obtained from alphaolefin polymerization followed by hydrogenation. Regarding nanomaterials, graphene derivatives are considered interesting nanoadditives for lubricants due to their abilities to improve base oils performances and their good stability in the lubricants against sedimentation over time [39]. h-BN, with lamellar crystalline structure [40], showed great performance when used as additive in lubricating oils [41,42]. Steel to steel contact was selected to carry out the tribological tests with the dispersions. These assays can help to identify the more efficient additives for lubricants. In addition, thermophysical properties of the lubricants were measured.

2. Materials and methods

2.1. Materials

Graphene nanoplatelets, hexagonal boron nitride, and the three phosphonium ILs, $[P_{6,6,6,14}][DEHP]$ (IL1), $[P_{2,4,4,4}][DEP]$ (IL2) and $[P_{6,6,6,14}][(iC8)_2PO_2]$ (IL3) (Fig. 1), were supplied by Iolitec whereas the base oil (polyalphaolefin 32, PAO), with a density of 0.8403 g cm^{-3} at 298.15 K and a dynamic viscosity of 236.0 mPa s at 313.15 K, was kindly provided by REPSOL. Table S1 shows more details of the used samples.

Scanning Electron Microscope (SEM) micrographs, X-ray patterns, EDX microanalyses and Raman spectrum of h-BN nanoparticles (disc like shape of nominal diameter of 70 nm with a layered hexagonal structure with an interlayer distance greater than 0.33 nm) were previously reported by Guimarey et al. [43] and Liñeira del Río et al. [41]. The EDX results showed that h-BN purity is approximately 99%. Graphene nanoplatelets, which were characterized (SEM, TEM, Raman and FTIR) by Liñeira del Río et al. [44], have a purity of 99.5%, a mean particle diameter of 15 μm and a thickness of 11–15 nm. Polyalphaolefin 32 was obtained mixing PAO 40 and PAO 6 in a proportion of 89/11 wt %, respectively. FTIR and Raman spectra of the three ionic liquids (IL1, IL2 and IL3) and PAO were previously reported by Nasser et al. [27], who identified all peaks and bands.

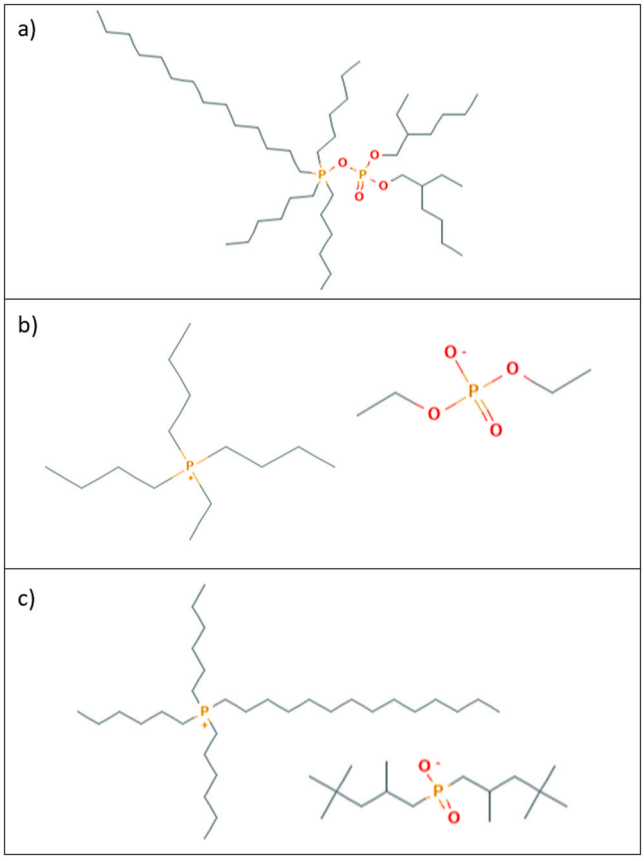

Fig. 1. Chemical structure of phosphonium ILs: a) $[P_{6,6,6,14}][DEHP]$ (IL1), b) $[P_{2,4,4,4}][DEP]$ (IL2) and c) $[P_{6,6,6,14}][(iC8)_2PO_2]$ (IL3).

2.2. Sampling preparation

The nano-lubricants PAO/*a* wt% h-BN and PAO/*b* wt% GnP, being *a* 0.025, 0.05 or 0.1 and *b* 0.025, were prepared using the two-step method. From tribological results (see Section 3.1 and Nasser et al. [29]) *a*= 0.1 and *b*= 0.05 were selected. Subsequently, four dispersions were made: PAO/0.1 wt% h-BN/0.05 wt% GnP and PAO/1 wt% ILX/0.1 wt% h-BN/0.05 wt% GnP (X = 1, 2 or 3). For the last three nanodispersions, adequate amounts of GnP and h-BN nanopowders were added to each ionic liquid in an agate mortar, then melded with the pestle in continuous motion for 10 min, to obtain the three heterogeneous blends: 1 wt% ILX (X = 1, 2 or 3)/0.1 wt% h-BN/0.05 wt% GnP. Subsequently, each blend is added to the appropriate amount of PAO oil obtaining the final PAO/1 wt% ILX/0.1 wt% h-BN/0.05 wt% GnP dispersions. 1 wt% of ILs concentration was selected according to the Zhou and Qu [22] review. The mass concentrations of h-BN, GnP and ILs were determined using a Sartorius MC 210 P high precision balance (0.00001 g).

After preparation, all samples were continuously sonicated in a Fisherbrand TM 11203 ultrasonic bath at 37 kHz of frequency and an effective power of 180 W for 4 h, to obtain homogeneous nano-lubricants. Two sets of nanodispersions were arranged, one to analyze the stability of nano-lubricants by visual observation and the other to carry out tribological tests.

2.3. Thermophysical characterization

Densities and viscosities of the four nanodispersions were measured, at 0.1 MPa, in the range (278.15–373.15) K by means of an Anton Paar SVM 3000 rotational Stabinger viscometer. This apparatus consists of two cells, one for the density measurement and another for viscosity. Details of the device are reported in Table 1.

2.4. Tribological trials

A CSM Standard tribometer in the rotational ball-on-disc configuration was used to carry out the friction tests. The procedure was previously reported [29] and is summarized in Table 2.

Surface topography profiles of worn surfaces of the discs were obtained with a Sensofar S neox 3D Optical Profilometer. From these profiles, the width, cross sectional area and maximum depth were determined. A Scanning Electron Microscope (SEM, Carl Zeiss FESEM ULTRA Plus) was also used to characterize the worn surface topography. Confocal Raman microscopy (WITec alpha300R+) was used to understand the role that both ILs and nanomaterials have in the reduction of worn scars compared to those lubricated with PAO base oil, being 0.5 μm the depth of detection that this technique has with our samples under the measurement conditions.

3. Results and discussion

3.1. Concentration selection of nanoadditives

For the suitable concentration selection of nanoadditives (h-BN and GnP) in PAO, PAO/*a* wt% h-BN (*a* 0.025, 0.05 or 0.1 wt%) and PAO/0.025 wt% GnP dispersions were tested with the tribometer (Table S2). The friction coefficients (μ) with the nanodispersions PAO/0.05 wt% GnP and PAO/0.1 wt% GnP were previously reported [29]. Fig. 2 shows the friction values of these nanodispersions together with that of PAO. Respect to neat PAO, friction percentage reductions of 20%, 23% and 26% were achieved with the addition of 0.025, 0.05 and 0.1 wt% h-BN, respectively. Regarding the addition of 0.025, 0.05 and 0.1 wt% GnP to PAO the corresponding reductions were 15%, 17% and 5%. Consequently, concentrations 0.1 wt% h-BN and 0.05 wt% GnP were selected for further experiments herein. Hereafter, 0.05 wt% GnP/0.1 wt% h-BN will be referred to as GnP/h-BN.

3.2. Stability of the nanodispersions

All the samples were kept at room temperature with no disruption to detect if sedimentation occurs at the bottom of the vial or, conversely, the sample remains stable. The images are shown in Fig. 3. Partial sedimentation of nanodispersions including GnP/h-BN (Fig. 3a) and IL2/GnP/h-BN (Fig. 3c) was observed before 60 days of preparation, whereas no sedimentation occurs for the nanodispersions PAO/IL1/GnP/h-BN and PAO/IL3/GnP/h-BN, which remain stable for at least 150 days. Thus, regarding the temporal stability of the dispersions, positive synergies are revealed between IL1 $[P_{6,6,6,14}][DEHP]$ or IL3 $[P_{6,6,6,14}][(iC8)_2PO_2]$ and GnP/h-BN. Note that these two last ILs contain the same cation, $[P_{6,6,6,14}]^+$. Similar positive synergies were previously found for h-BN dispersions with the same ILs [27].

Table 1
Rotational Stabinger device details.

Anton Paar Stabinger SVM 3000		
Property	Operational principle	Expanded uncertainty (k = 2)
Temperature	Pt100	0.02 K from 288.15 K to 378.15 K 0.05 K outside that range
Density	Oscillating U-tube	0.0005 g cm^{-3}
Viscosity	Rotational Couette viscometer with cylindrical geometry	1%

Table 2
Test conditions and tribopairs.

CSM Standard tribometer: rotational ball-on-disc configuration				
Test parameters		Tribopair		
Normal load	20 N		Ball	Disc
Radius	3 mm	Material	AISI 52100	AISI 52100
Linear speed	0.1 $m{\cdot}s^{-1}$	Dimensions (mm)	∅6	∅10
Time	3400 s			
Lubricant volume	0.15 mL	Hardness	58–66 HRC	190–210 Hv30
Temperature	Room temperature	Surface roughness, Ra	–	< 0.02 μm

3.3. Thermophysical properties

The density (ρ) and the dynamic viscosity (η) of the four PAO dispersions are reported, in the range (278.15–373.15) K, in Tables S3 and S4. All nano-lubricants showed slightly greater density values than PAO. Fig. S1 presents, for each nanodispersion, the mean increase in the entire temperature range. Specifically, the density increase values due to the addition of GnP/h-BN nanomaterials without or with ILs range from 0.21% (PAO/GnP/h-BN at 373.15 K) to 0.46% (PAO/IL2/GnP/h-BN at 298.15 K).

Viscosity values of the dispersions are higher than those of PAO as can be seen in Fig. S2 and Table S4. Viscosity increases values due to GnP/h-BN nanomaterials without or with ILs addition range from 2.0% to 8.9%; the highest increase corresponds to the double hybrid nanodispersion containing IL2 at 278.15 K, and the minimum to PAO/GnP/h-BN at 373.15 K.

3.4. Friction behavior

The friction performance of all the lubricants is illustrated in Fig. 4, whereas Table S5 presents for each lubricant the average μ values (three replicates) together with their percentage reductions and standard deviations. All tested nanodispersions improve the friction behavior of the base oil. The friction reductions ranged from 33% to 40%, where the lowest reduction (33%) was achieved by addition of both 0.05 wt% GnP and 0.1 wt% h-BN to PAO, while their use separately as additives led to 26% and 17% [29], respectively (Fig. 2). This fact shows the relevance of their hybrid combination as additives and the synergies between both NPs. Slightly better results were obtained with the PAO/IL3/h-BN/GnP hybrid lubricant, followed by PAO/IL1/h-BN/GnP and then PAO/IL2/h-BN/GnP with friction reductions of 40%, 35% and 34% respectively. Therefore, positive anti-friction synergies were found when ILX is added to the PAO/GnP/h-BN nanodispersion. Comparing the results obtained for the double hybrid nanodispersions (PAO/ILX/GnP/h-BN) with those of PAO/ILX/GnP [29], positive synergistic effects were observed between the combination GnP/h-BN and each of the ILs based on $[P_{6,6,6,14}]^+$ (IL1 and IL3), as anti-friction PAO additives, especially with the nano-lubricant containing IL3. Furthermore, we must bear in mind that the hybrid combination containing IL2 does not improve the temporal stability of the PAO/GnP/h-BN dispersion. Previous results in PAO/ILX/h-BN [27] led to friction reductions of up to 17% compared to neat PAO and for PAO/ILX/GnP [29] these reductions reached 24%, whereas the double hybrid nanodispersions PAO/ILX/GnP/h-BN lead to friction improvements of up to 40%. Therefore, these results validate the positive synergies not only of the hybrid combination GnP/h-BN but also of the double hybrids (both nanomaterials and ILs).

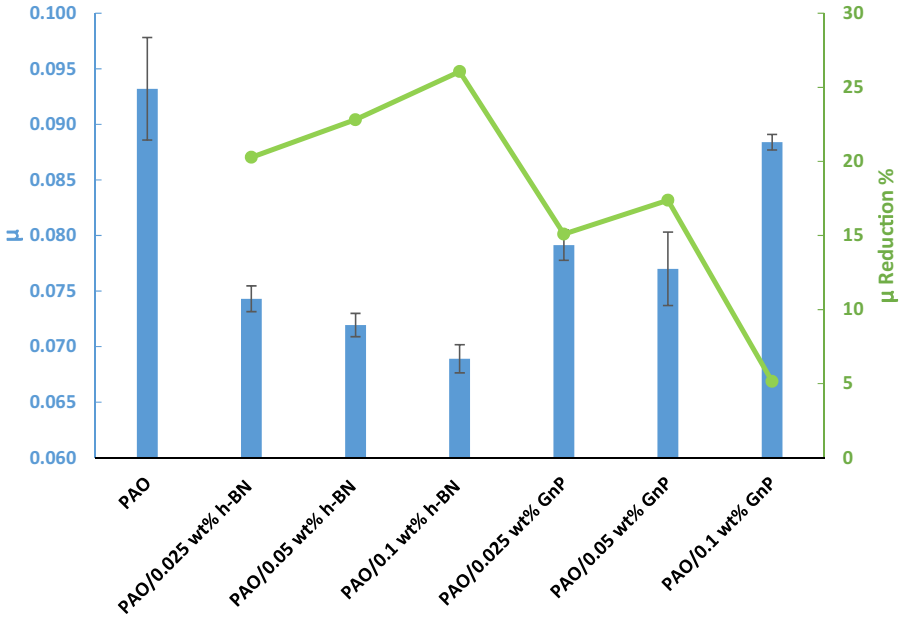

Fig. 2. Average friction coefficient (μ) of different nanodispersions compared with that of neat PAO (Table S2 and [29]).

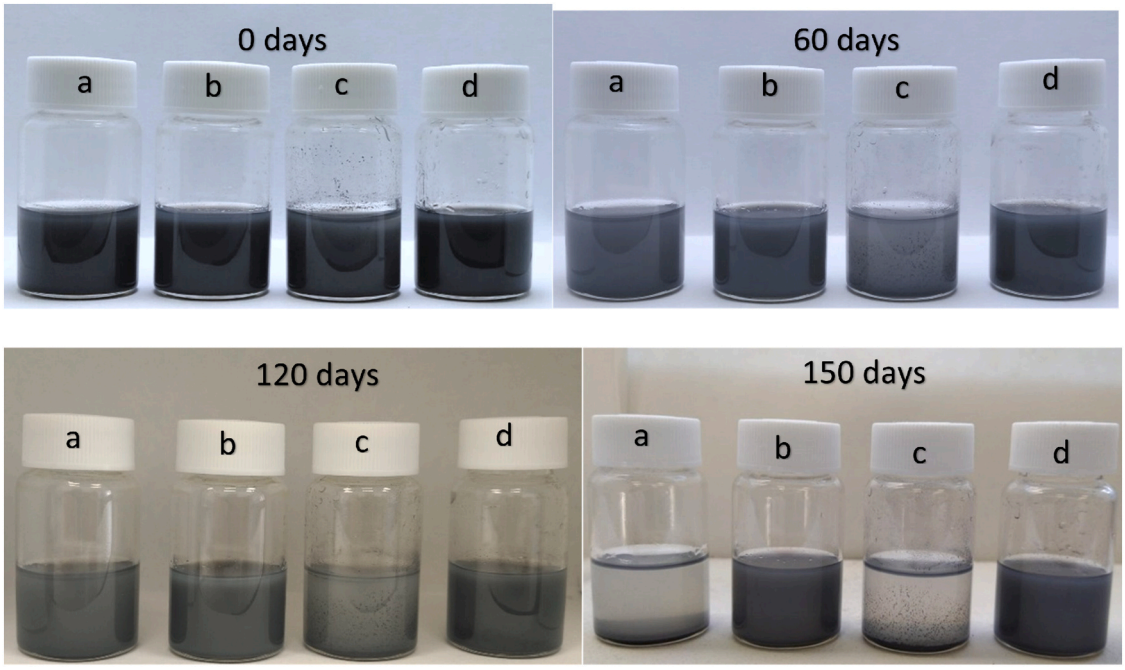

Fig. 3. Sample photos to monitor any precipitation of the additives in PAO lubricant oil; (a) PAO/GnP/h-BN, (b) PAO/IL1/GnP/h-BN, (c) PAO/IL2/GnP/h-BN, and (d) PAO/IL3/GnP/h-BN.

3.5. Wear behavior and analysis of the worn surface

The average values of the three replicates of the wear parameters measured (wear scar width, WSW, cross-sectional area, and the maximum depth of the wear track) are also reported in Table S5. Fig. 5 presents the WSW values of the discs lubricated with the designed lubricants, generated during the friction tests. Table S5 shows that the addition of 0.1 wt% h-BN/0.05 wt% GnP to PAO slightly reduces the WSW from 260.0 μm [29] to 246.7 μm. On the other hand, the hybrid combinations of 1 wt% IL1 or 1 wt% IL2 or 1 wt% IL3 with 0.1 wt% h-BN/0.05 wt% GnP resulted in significant reductions in WSW, down to 231.0 μm, leading to a reduction of 11%, whereas for the previously tested nano-lubricants 1% wt ILX/0.05 wt% GnP [29], without h-BN, similar width reductions were achieved (12%). Table S5 also shows reductions in the cross-sectional area for all the nanodispersions, ranging from 9%, in the case of PAO/h-BN/GnP, to 18% for PAO/IL2/h-BN/GnP and for PAO/IL1/h-BN/ GnP. As regards the worn scar depths, a similar trend was found. In this case, the wear reductions range from 13% to 16% for the same dispersions. As an example, in Fig. 6 the 2D wear track profiles corresponding to PAO/IL1/GnP/h-BN (in blue) and the neat PAO (in orange). Accordingly, comparable anti-wear results were found for the three hybrid nanodispersions containing ILs. Thus, comparing the wear results obtained for the double hybrid nanodispersions PAO/ILX/GnP/h-BN with those of

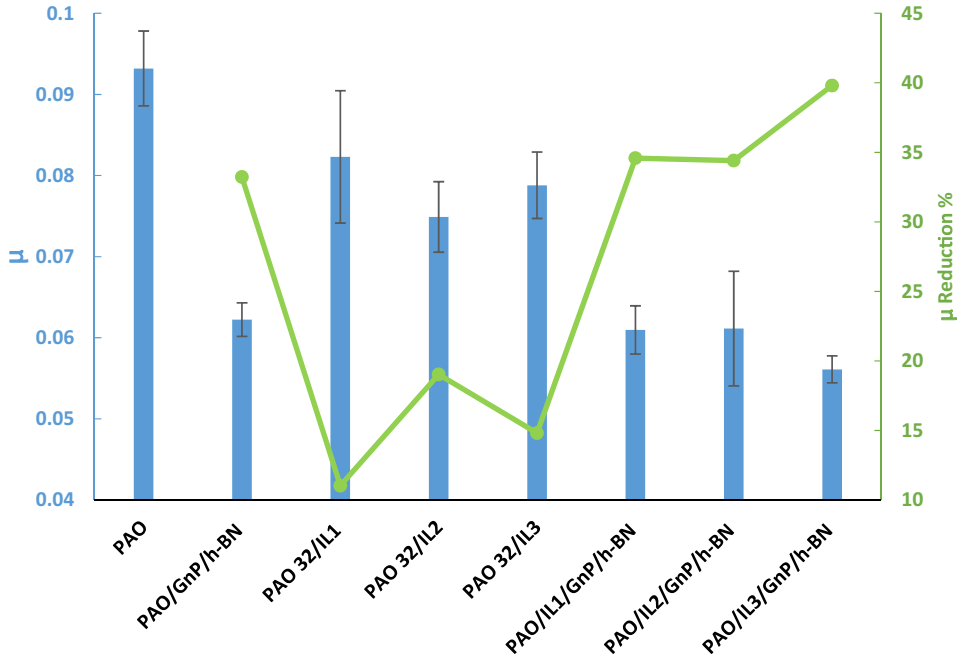

Fig. 4. Average friction coefficient values (μ, Table S5 and [29]) and their corresponding reductions for PAO/GnP/h-BN, PAO/ILX [29] and for PAO/ILX/ GnP/h-BN (X = 1, 2 or 3) compared with that of PAO base oil.

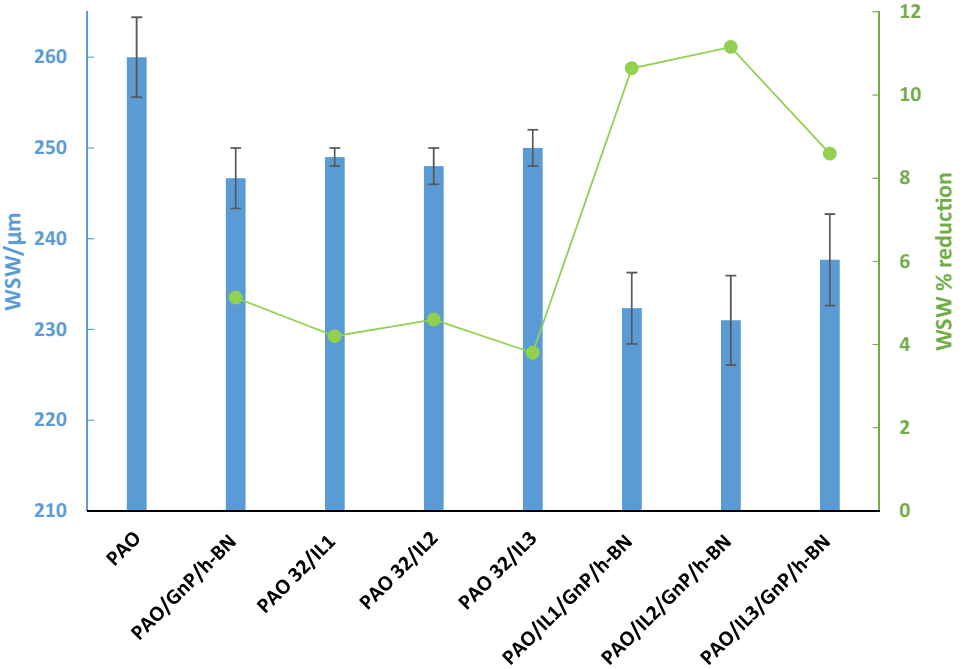

Fig. 5. Average WSW (μm) values (Table S5 and [29]) at the disc surfaces lubricated with different samples, and their reductions (%) respect to neat PAO performance (room temperature).

PAO/GnP/h-BN, positive synergistic effects were observed between the GnP/h-BN combination and each IL, as PAO anti-wear additives. Regarding the effect of adding h-BN NPs, the anti-wear behavior in terms of WSW using PAO/ILX/GnP/h-BN dispersions is similar to those obtained using PAO/ILX/GnP lubricants, although worse for the transversal area or the depth [29].

The roughness values (Ra) of worn disc surfaces, measured with the 3D optical profilometer (ISO 4287 standard, 0.08 mm Gaussian filter long wavelength cut-off), are shown in Fig. 7. Varied results were found depending on the type of lubricant, the lowest Ra (0.058 μm) corresponds to the addition of IL2/GnP/h-BN to PAO, leading to a reduction of 62% compared to the worn surface lubricated with the base oil, whose Ra is 0.151 μm. Moreover, the hybrid combination of GnP/h-BN and IL1 or IL3 resulted in the decrease of Ra to 0.071 μm and 0.062 μm, respectively, when added to PAO. Hence, it can be concluded that the smoothness of the worn surfaces is due to the presence of the nanoadditives and ILs. This fact again corroborates the existence of several positive synergistic effects between each of the ILs and GnP/h-BN.

Additionally, to analyze wear mechanisms, SEM micrographs of

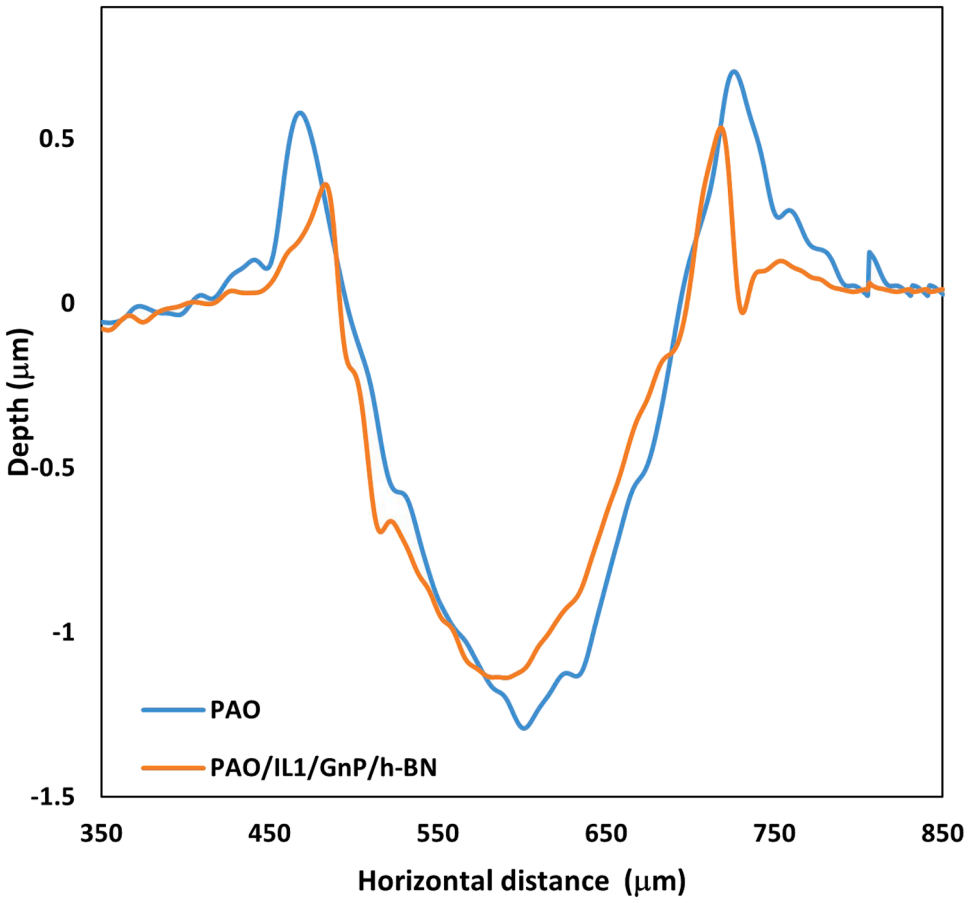

Fig. 6. Cross-sectional profiles of the worn tracks obtained with PAO and PAO/IL1/GnP/h-BN.

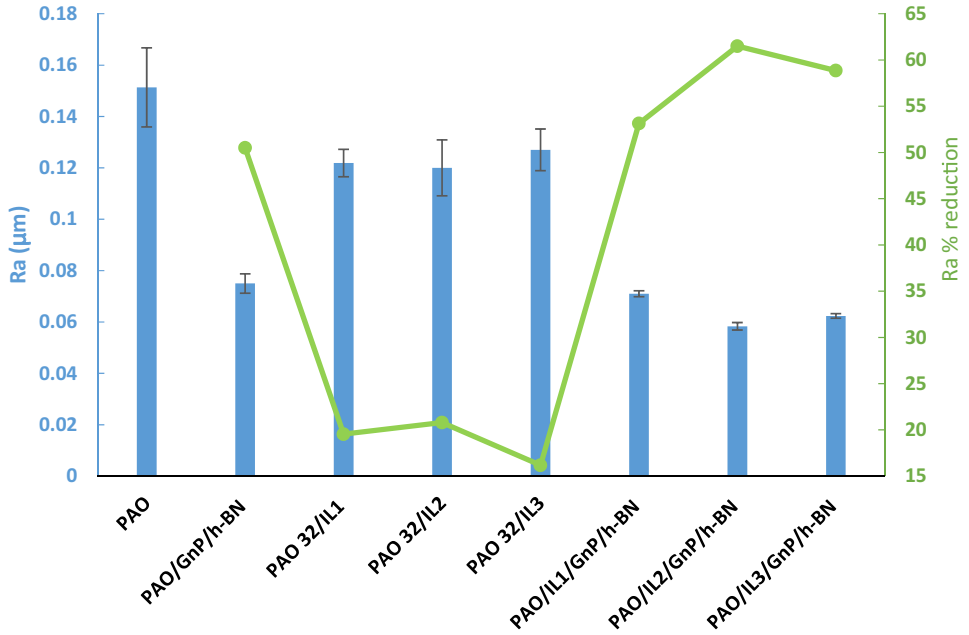

Fig. 7. Average Roughness values (Ra) at the worn surface of the discs lubricated by different dispersions. Ra values for neat PAO and PAO/ILX are reported in reference [29].

worn tracks lubricated with the studied lubricants were carried out. Fig. S3 shows that with the PAO/GnP/h-BN nano-lubricants and with the double hybrid nano-lubricants (PAO/ILX/GnP/h-BN) quite important decreases in WSW compared to that obtained with PAO base oil. These results confirm the WSW measurements obtained with the 3D profilometer (Table S5). Fig. S3 also evidences plastic deformation in all

the cases and abrasive wear scratches in the track corresponding to the neat PAO oil [29] whereas smoother surfaces were achieved for the tracks lubricated with the nano-lubricants. These results agree with the roughness measurements performed with the profilometer (Fig. 7).

Raman spectra and elemental mapping of the worn surfaces lubricated with PAO/GnP/h-BN (Fig. 8), and PAO/ILX/GnP/h-BN with X = 1, 2 or 3 (Figs. 8–10) were recorded with the confocal Raman microscope (wavelength 532 nm) to obtain information on the composition of the tribo-film. The Raman spectra of the nanodispersion components: PAO, IL1, IL2, IL3, and both nanoparticles were characterized in previous articles [27,28].

On the worn surface lubricated with PAO/GnP/h-BN, Fig. 8, Raman microscopy reveals areas containing GnP (cyan) and areas with h-BN (green). Regarding the worn scar lubricated with PAO/IL1/GnP/h-BN (Fig. 9) small areas with GnP and h-BN can also be observed (blue and green color, respectively). In addition, a significant tribo-film was found on the edges of the worn surface due to IL1 (cyan color).

Regarding the worn surface lubricated with PAO/IL2/GnP/h-BN (Fig. 10), an interface of a similar nature to the previous case was observed, i.e., there are small areas containing the nanoparticles (GnP and h-BN) and an IL tribo-film at the edges due to the presence of IL2. Finally, for the worn discs lubricated with PAO/IL3/GnP/h-BN (Fig. 11), the presence of areas of GnP and h-BN (cyan and green color, respectively) can be observed. However, on this surface, the number of h-BN small areas at the edges of the worn scar is strongly greater than in the previous cases. A significant IL3 tribo-film was detected at the edges of the worn surface as for the previous nanodispersions. It is interesting to note that for the nano-lubricants PAO/ILX/GnP/h-BN, no iron oxides were detected in the corresponding worn scars whereas for PAO/GnP/h-BN, ferrous oxide was found.

In summary, considering these Raman studies for all the worn surfaces lubricated with the prepared nanodispersions, as well as the roughness analysis of disc worn scars with the profilometer (Fig. 6), it can be concluded that the main tribological mechanisms are the formation of the IL tribo-films, as well as the mending/repairing effect due to nanoadditives (GnP and h-BN). Tribo-films generated in a steel–steel contact lubricated by an engine oil additivated with IL1 were detected by Zhou et al. [45]. Regarding the mending effect of nanoparticles, previous studies [27,28] showed that both h-BN and GnP nanoadditives tend to bind to the worn scar through the repairing tribological mechanism, improving the anti-friction and anti-wear performance as well as the roughness of the worn surface, as in this work. In the case of graphene nanoplatelets, this mechanism could be due to the extremely thin laminated structure, which offers low shear strength between the layers, avoiding interaction at the rubbing interface [46]. Furthermore, the planar shape of GnP gives them a lower probability of incising and deforming the asperities of shearing surfaces. In fact, Zhao et al. [47] analyzed the lubrication behavior for graphene nanoadditives with different exfoliations, concluding that tribological improvement is due to the formation of well-ordered graphene tribo-films at the friction interface and due to changes in the graphene microstructure during tribological tests. Considering these results, positive anti-friction and anti-wear synergies were found between the GnP/h-BN nanoadditives and the IL with the hybrid nanodispersions.

4. Conclusions

In this work, synergistic effects of h-BN nanoparticles and GnP nanoplatelets with or without ILX (X = 1, 2 or 3) as additives of PAO base oil for an AISI 52100/AISI 52100 contact pair at room temperature were studied and the following achievements have been reached:

- Based on friction tests, the concentrations 0.1 wt% h-BN and 0.05 wt % GnP were selected in this article. As regards ILs, the concentration was 1 wt%.
- From the four dispersions (PAO/GnP/h-BN and PAO/ILX/GnP/h-BN, X = 1, 2 or 3) those containing IL1 and IL3 were stable for at least 150 days whereas sedimentation appears in the other two before 60 days.
- The base oil density increments due to the addition of h-BN and GnP without or with ILs ranges from 0.21% to 0.46%, whereas the

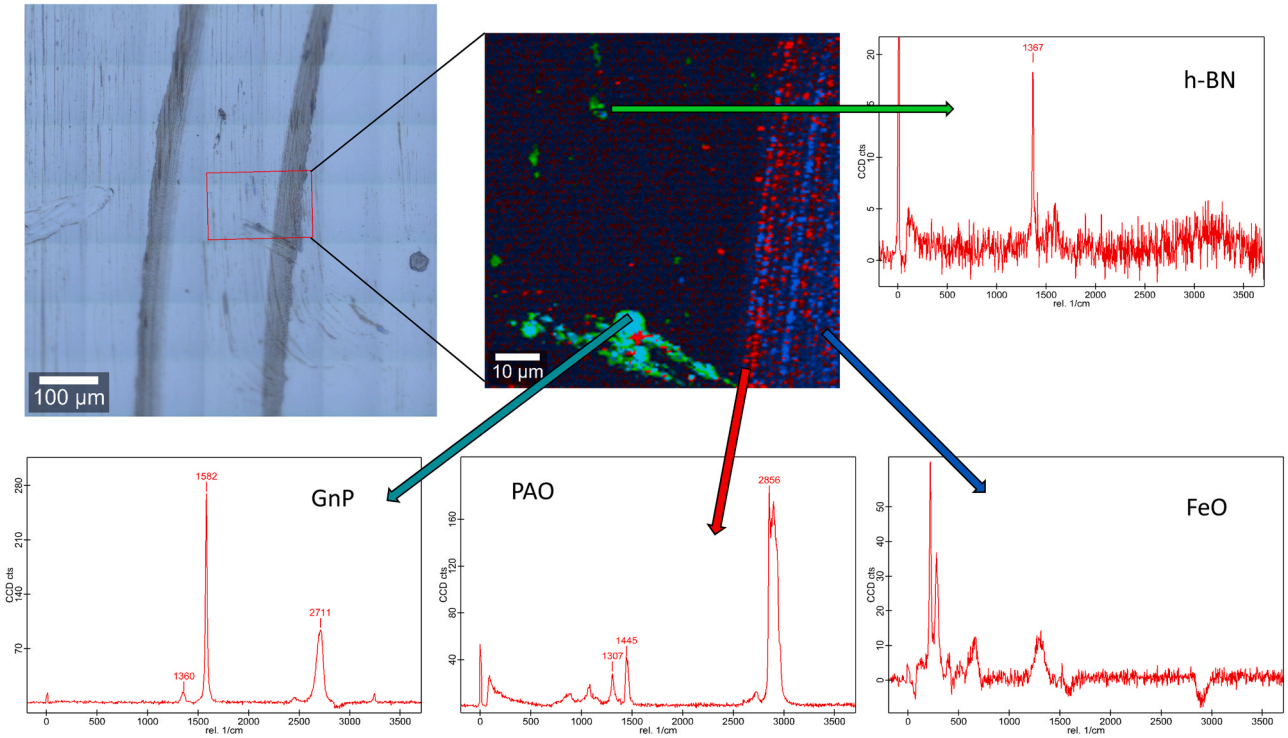

Fig. 8. Raman spectra and elemental map of the worn surface corresponding to the nano-lubricant PAO/GnP/h-BN.

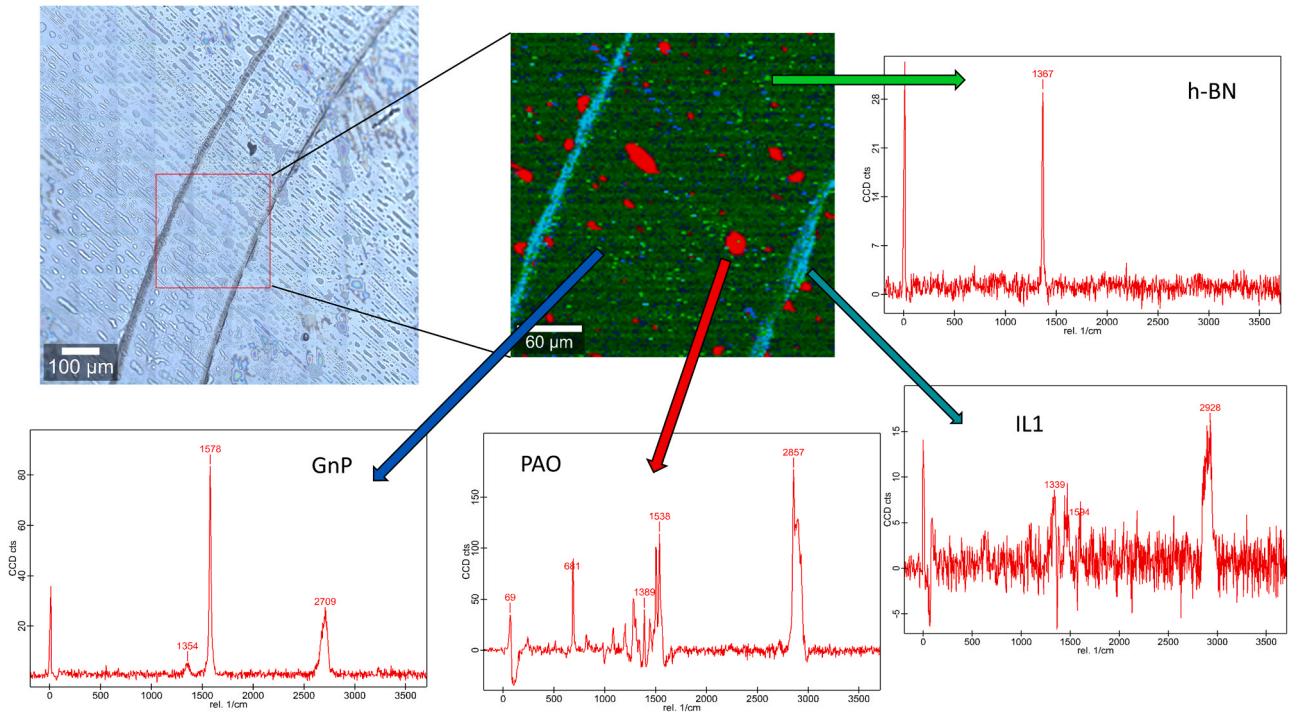

Fig. 9. Raman spectra and elemental map of the worn surface corresponding to the nano-lubricant PAO/IL1/GnP/h-BN.

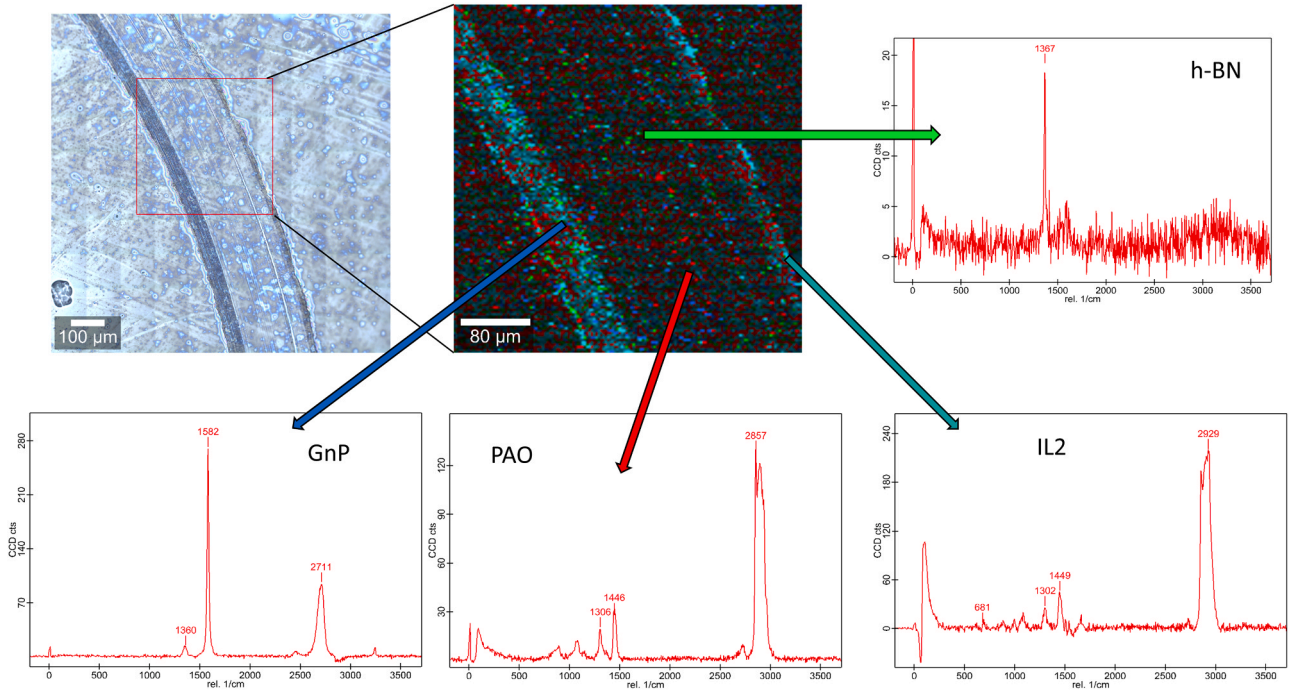

Fig. 10. Raman spectra and elemental map of the worn surface corresponding to the nano-lubricant PAO/IL2/GnP/h-BN.

viscosity ones reach 8.9%. The maximum increases for both properties correspond to the nanodispersion PAO/IL2/GnP/h-BN.

- All nanodispersions improve both the anti-friction and anti-wear capabilities of PAO. Friction reductions ranged from 33% to 40%, being the best anti-friction behavior for the nano-lubricant PAO/IL3/h-BN/GnP. As regards wear, reductions in terms of WSW ranged from 5% to 11%, being the best anti-wear performance for the PAO/IL2/GnP/h-BN and PAO/IL1/GnP/h-BN nanolubricants. Tribo-film formation due to ILs and mending effect due to nanoparticles were confirmed by roughness measurements and confocal Raman microscopy on the worn surfaces.
- From the above results, it can be concluded that positive synergies in terms of stability, anti-friction capability and worn surface roughness were found between the ILs containing the trihexyltetradecylphosphonium cation and both GnP and h-BN as hybrid additives of PAO. Furthermore, it should be noted that there are no anti-wear improvements when h-BN is added to PAO/ILX/GnP nanodispersions. Nevertheless, there is an important improvement in

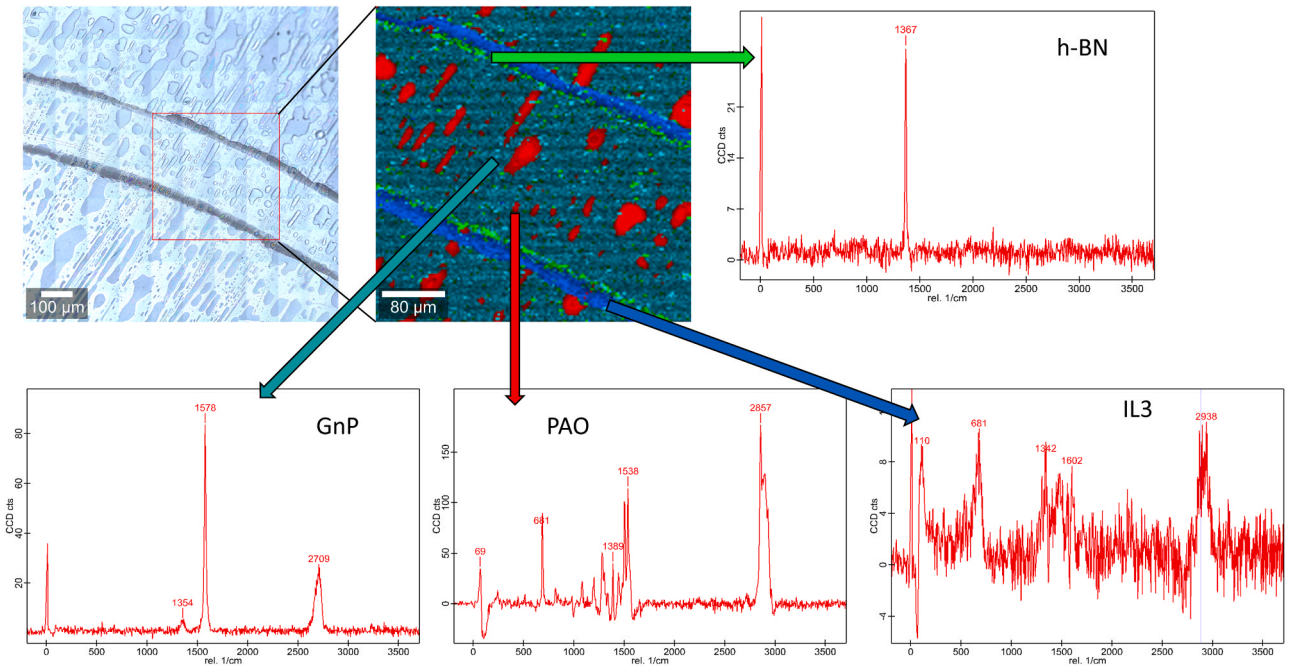

Fig. 11. Raman spectra and elemental map of the worn surface corresponding to the nano-lubricant PAO/IL3/GnP/h-BN.

the worn surface roughness when PAO/ILX/GnP/h-BN (X = 1, 2 or 3) is used as lubricant.

CRediT authorship contribution statement

Khodor Nasser: Validation, Formal analysis, Writing – original draft, Visualization. **José M. Liñeira del Río:** Formal analysis, Writing – review & editing. **Fátima Mariño:** Formal analysis, Writing – review & editing. **Enriqueta R. López:** Methodology, Formal analysis, Supervision, Writing – review & editing. **Josefa Fernández:** Conceptualization, Writing – review & editing, Supervision, Project administration.

Declaration of Competing Interest

The authors declare that they have no known competing financial interests or personal relationships that could have appeared to influence the work reported in this paper.

Acknowledgments

Authors thank Repsol for supplying us the PAO sample. Authors acknowledge the use of the RIAIDT-USC analytical facilities, particularly to Mr. Ezequiel Vázquez for his valuable guidance. Ministry of Science and Innovation (Spain) and the European Regional Development Fund supported this work through the project ENE2017-86425-C2-2-R. This research was also financially supported by Xunta de Galicia, Spain (Grant ED431C 2020/10).

Appendix A. Supporting information

Supplementary data associated with this article can be found in the online version at doi:10.1016/j.triboint.2021.107189.

References

[1] Holmberg K, Erdemir A. Influence of tribology on global energy consumption, costs and emissions. Friction 2017;5:263–84. https://doi.org/10.1007/s40544-017-0183-5.

[2] Holmberg K, Erdemir A. The impact of tribology on energy use and CO_2 emission globally and in combustion engine and electric cars. Tribol Int 2019;135:389–96. https://doi.org/10.1016/j.triboint.2019.03.024.

[3] Holmberg K, Kivikytö-Reponen P, Härkisaari P, Valtonen K, Erdemir A. Global energy consumption due to friction and wear in the mining industry. Tribol Int 2017;115:116–39. https://doi.org/10.1016/j.triboint.2017.05.010.

[4] He F, Xie G, Luo J. Electrical bearing failures in electric vehicles. Friction 2020;8:4–28. https://doi.org/10.1007/s40544-019-0356-5.

[5] Bondarev AV, Fraile A, Polcar T, Shtansky DV. Mechanisms of friction and wear reduction by h-BN nanosheet and spherical W nanoparticle additives to base oil: experimental study and molecular dynamics simulation. Tribol Int 2020;151:106493. https://doi.org/10.1016/j.triboint.2020.106493.

[6] Uflyand IE, Zhinzhilo VA, Burlakova VE. Metal-containing nanomaterials as lubricant additives: state-of-the-art and future development. Friction 2019;7:93–116. https://doi.org/10.1007/s40544-019-0261-y.

[7] Demas NG, Timofeeva EV, Routbort JL, Fenske GR. Tribological effects of BN and MoS_2 nanoparticles added to polyalphaolefin oil in piston skirt/cylinder liner tests. Tribol Lett 2012;47:91–102. https://doi.org/10.1007/s11249-012-9965-0.

[8] Liñeira del Río JM, López ER, González Gómez M, Yáñez Vilar S, Piñeiro Y, Rivas J, et al. Tribological behavior of nanolubricants based on coated magnetic nanoparticles and trimethylolpropane trioleate base oil. Nanomaterials 2020;10:683. https://doi.org/10.3390/nano10040683.

[9] Lee C-G, Hwang Y-J, Choi Y-M, Lee J-K, Choi C, Oh J-M. A study on the tribological characteristics of graphite nano lubricants. Int J Precis Eng Manuf 2009;10:85–90. https://doi.org/10.1007/s12541-009-0013-4.

[10] Kong L, Sun J, Bao Y. Preparation, characterization and tribological mechanism of nanofluids. RSC Adv 2017;7:12599–609. https://doi.org/10.1039/C6RA28243A.

[11] Gulzar M, Masjuki HH, Kalam MA, Varman M, Zulkifli NWM, Mufti RA, et al. Tribological performance of nanoparticles as lubricating oil additives. J Nanopart Res 2016;18:223. https://doi.org/10.1007/s11051-016-3537-4.

[12] Padgurskas J, Rukuiza R, Prosyčevas I, Kreivaitis R. Tribological properties of lubricant additives of Fe, Cu and Co nanoparticles. Tribol Int 2013;60:224–32. https://doi.org/10.1016/j.triboint.2012.10.024.

[13] Kumara C, Leonard DN, Meyer HM, Luo H, Armstrong BL, Qu J. Palladium nanoparticle-enabled ultrathick tribofilm with unique composition. ACS Appl Mater Interfaces 2018;10:31804–12. https://doi.org/10.1021/acsami.8b11213.

[14] Murthy N, Rai AK, Berkebile S. Improved loss-of-lubrication performance with lubricants containing nano-graphene platelets and ionic liquids. Appl Sci 2020;10:7958. https://doi.org/10.3390/app10227958.

[15] Zhao J, Huang Y, He Y, Shi Y. Nanolubricant additives: a review. Friction 2021;9:891–917. https://doi.org/10.1007/s40544-020-0450-8.

[16] Somers AE, Howlett PC, MacFarlane DR, Forsyth M. A review of ionic liquid lubricants. Lubricants 2013;1:3–21. https://doi.org/10.3390/lubricants1010003.

[17] Bermúdez M-D, Jiménez A-E, Sanes J, Carrión F-J. Ionic liquids as advanced lubricant fluids. Molecules 2009;14:2888–908. https://doi.org/10.3390/molecules14082888.

[18] Jiménez AE, Bermúdez MD, Iglesias P, Carrión FJ, Martínez-Nicolás G. 1-N-alkyl-3-methylimidazolium ionic liquids as neat lubricants and lubricant additives in steel–aluminium contacts. Wear 2006;260:766–82. https://doi.org/10.1016/j.wear.2005.04.016.

[19] Qu J, Blau PJ, Dai S, Luo H, Meyer HM. Ionic liquids as novel lubricants and additives for diesel engine applications. Tribol Lett 2009;35:181–9. https://doi.org/10.1007/s11249-009-9447-1.
[20] Otero I, López ER, Reichelt M, Villanueva M, Salgado J, Fernández J. Ionic liquids based on phosphonium cations as neat lubricants or lubricant additives for a steel/steel contact. ACS Appl Mater Interfaces 2014;6:13115–28. https://doi.org/10.1021/am502980m.
[21] Zhou Y, Qu J. Ionic liquids as lubricant additives: a review. ACS Appl Mater Interfaces 2017;9:3209–22. https://doi.org/10.1021/acsami.6b12489.
[22] Rivera N, Blanco D, Viesca JL, Fernández-González A, González R, Hernández Battez A. Tribological performance of three fatty acid anion-based ionic liquids (FAILs) used as lubricant additive. J Mol Liq 2019;296:111881. https://doi.org/10.1016/j.molliq.2019.111881.
[23] Gutierrez MA, Haselkorn M, Iglesias P. The lubrication ability of ionic liquids as additives for wind turbine gearboxes oils. Lubricants 2016;4:14. https://doi.org/10.3390/lubricants4020014.
[24] Vallejo JP, Liñeira del Río JM, Fernández J, Lugo L. Tribological performance of silicon nitride and carbon black Ionanofluids based on 1-ethyl-3-methylimidazolium methanesulfonate. J Mol Liq 2020;319:114335. https://doi.org/10.1016/j.molliq.2020.114335.
[25] Sanes J, Avilés M-D, Saurín N, Espinosa T, Carrión F-J, Bermúdez M-D. Synergy between graphene and ionic liquid lubricant additives. Tribol Int 2017;116:371–82. https://doi.org/10.1016/j.triboint.2017.07.030.
[26] Senatore A, Pisaturo M, Guida D. Polyalkylene glycol based lubricants and tribological behaviour: role of ionic liquids and graphene oxide as additives. J Nanosci Nanotechnol 2018;18:913–24. https://doi.org/10.1166/jnn.2018.15253.
[27] Nasser KI, Liñeira del Río JM, López ER, Fernández J. Synergistic effects of hexagonal boron nitride nanoparticles and phosphonium ionic liquids as hybrid lubricant additives. J Mol Liq 2020;311:113343. https://doi.org/10.1016/j.molliq.2020.113343.
[28] Liñeira del Río JM, López ER, Fernández J. Synergy between boron nitride or graphene nanoplatelets and tri(butyl)ethylphosphonium diethylphosphate ionic liquid as lubricant additives of triisotridecyltrimellitate oil. J Mol Liq 2020;301:112442. https://doi.org/10.1016/j.molliq.2020.112442.
[29] Nasser KI, Liñeira del Río JM, López ER, Fernández J. Hybrid combinations of graphene nanoplatelets and phosphonium ionic liquids as lubricant additives for a polyalphaolefin. J Mol Liq 2021;336:116266. https://doi.org/10.1016/j.molliq.2021.116266.
[30] Upendra M, Vasu V. Synergistic effect between phosphonium-based ionic liquid and three oxide nanoparticles as hybrid lubricant additives. J Tribol 2020;142:052101. https://doi.org/10.1115/1.4045769.
[31] Li Y, Zhang S, Ding Q, Li H, Qin B, Hu L. Understanding the synergistic lubrication effect of 2-mercaptobenzothiazolate based ionic liquids and Mo nanoparticles as hybrid additives. Tribol Int 2018;125:39–45. https://doi.org/10.1016/j.triboint.2018.04.019.
[32] Xie H, Dang S, Jiang B, Xiang L, Zhou S, Sheng H, et al. Tribological performances of SiO_2/graphene combinations as water-based lubricant additives for magnesium alloy rolling. Appl Surf Sci 2019;475:847–56. https://doi.org/10.1016/j.apsusc.2019.01.062.
[33] Song W, Yan J, Ji H. Fabrication of GNS/MoS_2 composite with different morphology and its tribological performance as a lubricant additive. Appl Surf Sci 2019;469:226–35. https://doi.org/10.1016/j.apsusc.2018.10.266.
[34] Sharma AK, Tiwari AK, Dixit AR, Singh RK, Singh M. Novel uses of alumina/graphene hybrid nanoparticle additives for improved tribological properties of lubricant in turning operation. Tribol Int 2018;119:99–111. https://doi.org/10.1016/j.triboint.2017.10.036.
[35] Vardhaman BSA, Amarnath M, Ramkumar J, Mondal K. Enhanced tribological performances of zinc oxide/MWCNTs hybrid nanomaterials as the effective lubricant additive in engine oil. Mater Chem Phys 2020;253:123447. https://doi.org/10.1016/j.matchemphys.2020.123447.
[36] Monge R, González R, Hernández Battez A, Fernández-González A, Viesca JL, García A, et al. Ionic liquids as an additive in fully formulated wind turbine gearbox oils. Wear 2015;328–329:50–63. https://doi.org/10.1016/j.wear.2015.01.041.
[37] Michaelis K, Höhn B-R, Hinterstoißer M. Influence factors on gearbox power loss. Ind Lubr Tribol 2011;63:46–55. https://doi.org/10.1108/00368791111101830.
[38] Murphy WR, Blain DA, Galiano-Roth AS, Galvin PA. Benefits of synthetic lubricants in industrial applications. J Synth Lubr 2002;18:301–25. https://doi.org/10.1002/jsl.3000180406.
[39] Rasheed AK, Khalid M, Rashmi W, Gupta TCSM, Chan A. Graphene based nanofluids and nanolubricants – review of recent developments. Renew Sustain Energy Rev 2016;63:346–62. https://doi.org/10.1016/j.rser.2016.04.072.
[40] Kimura Y, Wakabayashi T, Okada K, Wada T, Nishikawa H. Boron nitride as a lubricant additive. Wear 1999;232:199–206. https://doi.org/10.1016/S0043-1648(99)00146-5.
[41] Liñeira del Río JM, Guimarey MJG, Comuñas MJP, López ER, Prado JI, Lugo L, et al. Tribological and thermophysical properties of environmentally-friendly lubricants based on trimethylolpropane trioleate with hexagonal boron nitride nanoparticles as an additive. Coatings 2019;9:509. https://doi.org/10.3390/coatings9080509.
[42] Biswal J, Pant HJ, Thakre GD, Sharma SC, Gupta AK. Evaluation of anti-wear properties of automobile lubricant with different additives using thin layer activation technique. J Radioanal Nucl Chem 2020;325:795–800. https://doi.org/10.1007/s10967-020-07146-0.
[43] Guimarey MJG, Comuñas MJP, López ER, Amigo A, Fernández J. Thermophysical properties of polyalphaolefin oil modified with nanoadditives. J Chem Thermodyn 2019;131:192–205. https://doi.org/10.1016/j.jct.2018.10.035.
[44] Liñeira del Río JM, Guimarey MJG, Comuñas MJP, López ER, Amigo A, Fernández J. Thermophysical and tribological properties of dispersions based on graphene and a trimethylolpropane trioleate oil. J Mol Liq 2018;268:854–66. https://doi.org/10.1016/j.molliq.2018.07.107.
[45] Zhou Y, Leonard DN, Guo W, Qu J. Understanding tribofilm formation mechanisms in ionic liquid lubrication. Sci Rep 2017;7:8426. https://doi.org/10.1038/s41598-017-09029-z.
[46] Liu L, Zhou M, Li X, Jin L, Su G, Mo Y, et al. Research progress in application of 2D materials in liquid-phase lubrication system. Materials 2018;11:1314. https://doi.org/10.3390/ma11081314.
[47] Zhao J, Mao J, Li Y, He Y, Luo J. Friction-induced nano-structural evolution of graphene as a lubrication additive. Appl. Surf. Sci. 2018;434:21–7. https://doi.org/10.1016/j.apsusc.2017.10.119.